GA–A27396

ROLE OF PLASMA RESPONSE IN NON-AXISYMMETRIC TOKAMAK EDGE DISPLACEMENTS

by
N.M. FERRARO, L.L. LAO, T.E. EVANS, R.A. MOYER, R. NAZIKIAN, D.M. ORLOV, M.W. SHAFER, and E.A. UNTERBERG

SEPTEMBER 2012

GENERAL ATOMICS

DISCLAIMER

GA–A27396

ROLE OF PLASMA RESPONSE IN NON-AXISYMMETRIC TOKAMAK EDGE DISPLACEMENTS

by
N.M. FERRARO, L.L. LAO, T.E. EVANS, R.A. MOYER,* R. NAZIKIAN,† D.M. ORLOV,*
M.W. SHAFER,‡ and E.A. UNTERBERG‡

This is a preprint of a paper to be presented at the Twenty-fourth IAEA Fusion Energy Conf., October 8-13, 2012 in San Diego, California.

*University of California San Diego, La Jolla, California, USA.
†Princeton Plasma Physics Laboratory, Princeton, New Jersey, USA.
‡Oak Ridge National Laboratory Oak Ridge, Tennessee, USA.

Work supported in part by
the U.S. Department of Energy
under DE-FG02-95ER54309, DE-FC02-04ER54698, DE-FG02-05ER54809,
DE-AC02-09CH11466, and DE-AC05-00OR22725

GENERAL ATOMICS PROJECT 03726
SEPTEMBER 2012

Role of Plasma Response in Non-Axisymmetric Tokamak Edge Displacements

N.M. Ferraro 1), L.L. Lao 1), T.E. Evans 1), R.A. Moyer 2), R. Nazikian 3), D.M. Orlov 2), M.W. Shafer 4), and E.A. Unterberg 4)

1) General Atomics, PO Box 85608, San Diego, CA 92186-5608, USA.
2) University of California San Diego, 9500 Gilman Drive, La Jolla, CA 92093-0417, USA.
3) Princeton Plasma Physics Laboratory, PO Box 451, Princeton, NJ 08543-0451, USA.
4) Oak Ridge National Laboratory, PO Box 2008, Oak Ridge, TN 37831, USA.

e-mail contact of main author: ferraro@fusion.gat.com

Abstract. Two-fluid, resistive modeling of plasma response to applied non-axisymmetric fields shows significant displacement of edge temperature and density profiles. The calculated displacements, often of two centimeters or more in H-mode pedestals with parameters appropriate to DIII-D, are due to the helical distortions resulting from stable edge modes being driven to finite amplitude by the applied fields. At low toroidal mode numbers (particularly $n = 1$ and $n = 2$) these displacements are greater in magnitude, and typically different in phase, than the distortions of the separatrix manifolds predicted from vacuum modeling. Comparison of these results finds good agreement with experimental measurements from Thomson scattering and soft x-ray imaging. In particular, the poloidal structures measured by x-ray imaging confirm that the plasma response is largely helical in nature, as opposed to simply a change in the axisymmetric transport properties. Additionally, modeling shows screening of islands in the H-mode pedestal, but island penetration near the top of the pedestal where the electron rotation vanishes. This may provide a mechanism for maintaining the pedestal width below values unstable to edge localized modes.

1. Introduction

The application of non-axisymmetric magnetic fields to tokamak plasmas is observed to affect the performance of the plasmas significantly, even when the non-axisymmetric fields are a small fraction ($\sim 10^{-4}$) of the axisymmetric fields present in the device. Judicious application of non-axisymmetric fields may improve plasma performance by supporting toroidal rotation of the plasma [1] (which is generally stabilizing), or by mitigating or suppressing edge-localized modes (ELMs) [2]. Potentially deleterious effects are also often observed, such as a strong reduction in plasma density [3, 4] ("pump-out"), a reduction in mode-locking thresholds [5], and substantial distortions of the plasma edge. In DIII-D, the peak-to-peak magnitude of these distortions, as measured by displacements of the temperature and density profiles, is typically of order 1 cm for typical ELM-suppression parameters with toroidal mode number $n = 3$, and may exceed 3 cm for $n = 1$ fields. For ITER, which has an outer gap of $\sim$5 cm [6], scaling the edge displacement with the linear dimensions of the device implies the possibility of direct contact of the plasma with the first wall.

Here, we calculate the temperature perturbations in the plasma edge from a linear two-fluid, resistive model using the M3D-C1 code [7]. It is shown that these calculated perturbations, which are essentially due to the displacement of magnetic surfaces, are in good agreement with experimental measurements. These perturbations are also found to be significantly enhanced by the plasma response to the non-axisymmetric fields in some cases, particularly at low toroidal mode number ($n = 1, 2$). In these cases, the calculated displacements may exceed the predictions of vacuum modeling by a factor of two or more [8]. We also show that two-fluid response results in screening in the H-mode pedestal, but may enhance the penetration of islands near the top of the pedestal. This provides a potential mechanism for constraining the pedestal width to a level that is stable to ELMs [9, 10].

2. Model

The model implemented in M3D-C1 includes the full plasma, separatrix, and scrape-off layer (SOL) within its computational domain. The region outside the separatrix is treated as a low temperature, low density plasma. Density, temperature, and current density vary smoothly across the separatrix. The fluid velocity and pressure perturbations are zero at the simulation domain boundary. The simulation domain boundary, illustrated in Fig. 1, is well outside of the plasma separatrix.

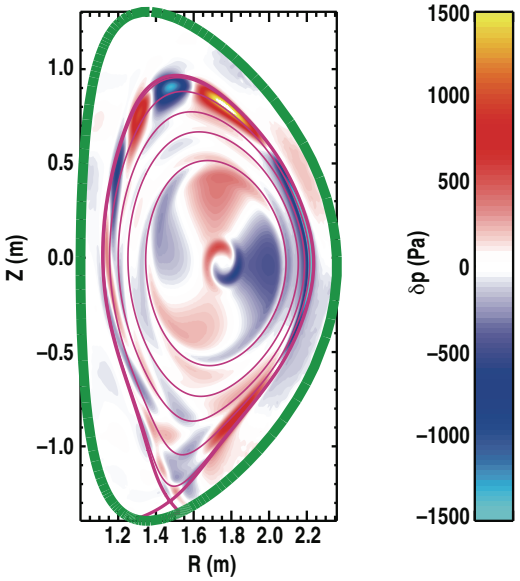

FIG. 1. The modeled pressure perturbation due to the linear plasma response to 2 kAt I-coil currents in an $n = 1$ configuration, using a reconstructed equilibrium from DIII-D discharge 117327. The thick green line indicates the simulation domain boundary. The magenta lines indicate the mode-rational surfaces with $q = 2$–6 and the separatrix.

The input to M3D-C1 includes the reconstructed Grad-Shafranov equilibria of the discharges to be analyzed, including axisymmetric electron temperature, electron density, and toroidal rotation profiles. In cases where equilibrium rotation is included, the equilibrium is self-consistently modified to take this rotation into account by including poloidal variations in the equilibrium pressure and density profiles. The currents in non-axisymmetric coils are also given as input. In the results presented here, the DIII-D I-coils are approximated as curved rectangles extending exactly 60° toroidally (whereas there are small toroidal gaps between coils in

reality). The non-axisymmetric fields produced by these idealized I-coils are calculated using the Biot-Savart law. The component of these fields normal to the simulation domain boundary is held fixed as a boundary condition for the plasma response calculation.

The linear plasma response is calculated using a time-independent, resistive, two-fluid model subject to these boundary conditions, as described in Ref. [7]. The outputs of the calculation are the perturbed density, pressure, velocity, and magnetic field of the given solution. The linear calculations presented here consider response of the same toroidal mode number as the applied field. The axisymmetric ($n = 0$) response is not considered here.

3. Results

In DIII-D, one may smoothly vary the phase of an applied $n = 1$ field from the I-coils, which have six coils toroidally. This admits the possibility to resolve the toroidal structure of the resulting non-axisymmetric equilibrium by rotating it past the diagnostics. This method was applied in DIII-D discharge 117327, in which $n = 1$ fields were applied with a 2 kAt amplitude current waveform in the I-coils. In this case, the waveform of the lower I-coil row was offset by 300 degrees from the upper row. The toroidal phase of this field (both upper and lower I-coil rows) was rotated at 5 Hz. The position of the pedestal top, Z_{ped}, shown as the black line in Fig. 2(a), was observed to oscillate at the same frequency as would be expected to be seen if a non-axisymmetric displacement were being rotated toroidally past the Thomson diagnostic. Z_{ped} is defined as one half-width within the center of a tanh fit of the Thomson electron temperature data along the Thomson chord (a vertical chord at $R = 1.94$ m). The value of this fit at the pedestal top, T_{ped}, is shown in Fig. 2(b). T_{ped} is roughly 700 eV, and does not oscillate with the frequency

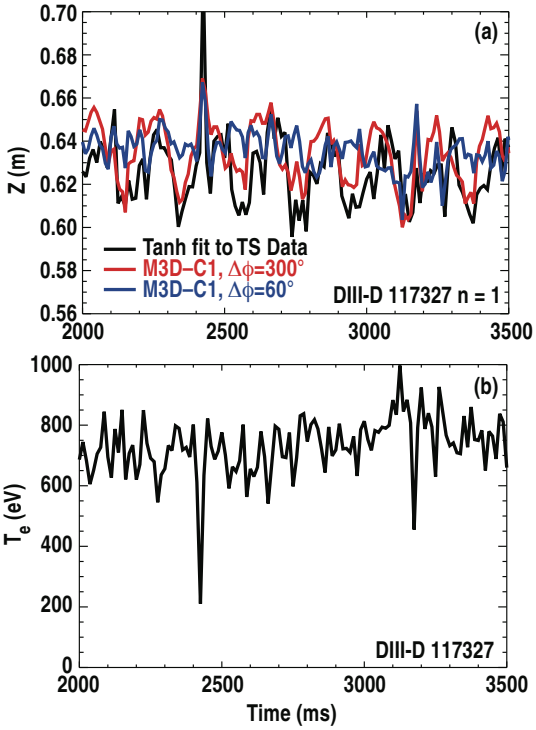

FIG. 2. (a) The measured (black line) and modeled (red line) position of the top of the pedestal in DIII-D discharge 117327 along the core Thomson chord as an $n = 1$ perturbation from the I-coils is rotated at 5 Hz. The modeled result changes significantly when the relative phases of the upper and lower I-coils are changed (blue line). The spikes at $t \approx 2400$ ms and $t \approx 3150$ ms are associated with ELMs. (b) The temperature of the pedestal top, T_{ped}, determined from a tanh *fit to the experimental data.*

of the applied field.

To provide the equilibrium used to model this shot, the equilibrium was reconstructed using pressure profiles obtained by averaging experimental data over several cycles of the applied field. The response was calculated by doing a single linear M3D-C1 calculation to obtain the phase and magnitude of the plasma response for a given I-coil phase. The predicted Z_{ped} at any time t is then obtained simply by multiplying this result by the appropriate phase factor, and determining where the resulting T_e profile along the Thomson chord equals $T_{ped}(t)$. This result is plotted versus time as the red line in Fig. 2(a), and is found to be in good agreement with the experimental results. In particular, both the phase and magnitude of the oscillation, which are not free parameters of the model, are found to be in good agreement.

In contrast, if the phase between the upper and lower I-coil rows is taken to be 60 degrees, instead of the experimental value of 300 degrees, the modeled result is found to be significantly different in phase and amplitude. This result is plotted as the blue line in Fig. 2(a).

Unlike $n = 1$ and $n = 2$ perturbations, the phase of $n = 3$ perturbations cannot be rotated smoothly using the DIII-D I-coil fields, which have 6 toroidal segments. Instead, the $n = 3$ response may be probed by reversing the I-coil currents, which is expected to have the effect of reversing the sign of the $n = 3$ plasma response (this is equivalent to a phase shift of 60 degrees). This procedure was carried out in DIII-D discharge 148712, by reversing the 4 kAt currents in the I-coils at 10 Hz. Thomson scattering measurements reveal a displacement of the edge T_e profile of 1–1.5 cm through much of the H-mode pedestal. These results are well reproduced by linear M3D-C1 calculations, which agree with the experimental displacements both in phase and magnitude through most of the pedestal (Fig. 3). There is some discrepancy near the pedestal top, where the M3D-C1 result overestimates the size of the displacement. The calculated response is large here due to the vanishing of the electron rotation frequency ω_e in this region [7, 11, 12]. The linear approximation used here is likely no longer valid in the vicinity of this large

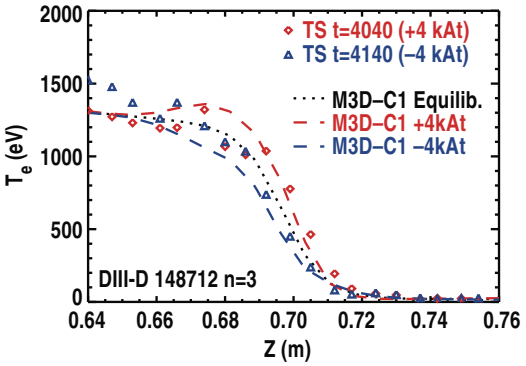

FIG. 3. The data points show the measurement of T_e from Thomson scattering, in the presence of a +4 kAt (red) and −4 kAt (blue) $n = 3$ current in the I-coils in DIII-D discharge 148712. The T_e profiles calculated by M3D-C1 in the presence of these applied fields are shown by the colored dashed lines. The black dotted line is the axisymmetric equilibrium input to M3D-C1.

response, as evidenced by the non-monotonic calculated temperature profile in the +4 kAt case.

The poloidal structure of the plasma response near the active x-point of DIII-D discharge 148712 is shown in Fig. 4. In this figure, the perturbed electron density calculated with M3D-C1 is compared with data from a soft x-ray diagnostic that has recently been installed on DIII-D [13]. The x-ray image is the difference between the signal averaged over a period with the I-coils in one phase and the signal averaged over a period with the I-coil current reversed. The x-ray emissivity of the plasma edge has not yet been fully characterized, but it is known to be a strong function of the electron density. A 3 μm beryllium filter on the detector excludes low-energy x-rays, with roughly 8% transmission at 500 eV and 72% transmission at 1 keV. Although this discharge is ELMing, the contribution to the averaged signal from x-rays emitted during ELMs is negligible small due to the infrequency and short duration of the ELMs.

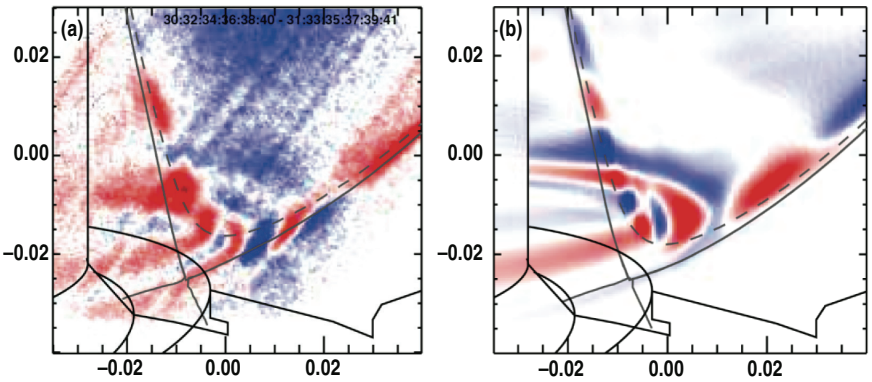

FIG. 4. (a) The measured perturbation soft x-ray emission in response to an $n = 3$ perturbation from the I-coils in DIII-D discharge 148712. (b) The simulated signal using temperature and density data from an M3D-C1 simulation of the same DIII-D discharge, using a model for x-ray emission. The dashed line represents the location of Ψ =0 .98.

In both the M3D-C1 and x-ray results, the edge response is seen to have a coherent and oscillatory poloidal structure. The poloidal structure in both results is consistent with a field-aligned mode structure in the edge. Both results also show strong radial localization, although it is not presently known to what extent the localization of the x-ray signal is due to the emissivity profile or the x-ray energy filtering, as opposed to the underlying mode structure.

Due to the large anisotropic thermal conductivity in these calculations ($\chi_\parallel/\chi_\perp \sim 10^6$), the displacements of the temperature profile are largely indicative of the displacements of the magnetic surfaces. However, due to the presence of resistivity, there is no guarantee that magnetic surfaces are preserved in the perturbed solution. Indeed, it is found that both magnetic islands and stochasticity exist in these solutions. With screening due

to plasma rotation [14], the islands are generally smaller than would be present if the perturbed fields were simply the applied fields (the "vacuum" fields). However, consistent with analytic theory [11, 15] and modeling [7, 12, 16], it is found that islands may be not be screened, and may even be amplified, in the region where the perpendicular electron frequency ω_e is small. An example of this is shown in Fig. 5. Here, the ω_e crosses zero near the $q = 8/3$ mode-rational surface at $\Psi \approx 0.85$, and the $m = 8$ island is found to be enhanced over the vacuum value. Even though islands at other mode-rational surfaces are still found to exist, they are screened sufficiently that some closed flux surfaces remain in the edge, and therefore radial diffusion from parallel transport is dramatically reduced below that from the vacuum fields. The result of these calculations is the prediction that the radial diffusion from parallel transport is not significant in the pedestal, but is significant at the top of the pedestal.

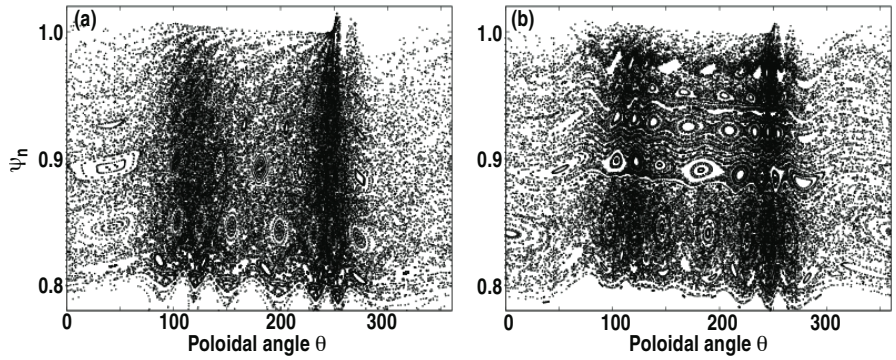

FIG. 5. Poincaré plots of the magnetic field given no plasma response (a) and two-fluid plasma response (b) to an applied $n = 3$ field. Plasma response reduces the island widths and stochasticity through most of the edge, except at the $q = 8/3$ surface, which is close to the location where $\omega_e = 0$.

4. Discussion

Linear, two-fluid calculations of plasma response to applied non-axisymmetric fields have been carried out with M3D-C1. The calculated displacements of edge temperature profiles are found to be in good agreement with experimental measurements from Thomson scattering and soft x-ray diagnostics, in both phase and magnitude. The degree to which the applied fields are resonant with the plasma response is found to have a significant effect on the amplitude of the displacements. Furthermore, the 3–4 cm peak-to-peak displacement found in the $n = 1$ case contrasts significantly with the calculated displacement of the separatrix manifolds due to the vacuum fields, which is less than one centimeter in this case. These results underscore the importance of the plasma response in the determining edge displacements. In the $n = 3$ case, the displacement calculated

from plasma response modeling is much closer in magnitude to the vacuum separatrix manifold displacement [17].

It has also been shown here that the plasma response typically acts to screen islands in the edge, significantly reducing stochasticity there. This screening resolves the apparent contradiction between vacuum modeling, which predicts significant radial diffusion of heat in the edge by parallel transport along stochastic field lines, and experiments, which see no reduction of the temperature gradient upon application of magnetic perturbations. An exception to the screening effect occurs in regions where ω_e is small ($\sim$10 krad/s or less). In co-rotating plasmas, this region typically exists near the top of the H-mode pedestal, whereas in counter-rotating plasmas this condition is usually never met. This stochastization at the top of the pedestal is consistent with emerging experimental results [10], and may provide a mechanism for limiting the width of the pedestal to levels that are not unstable to ELMs in co-rotating plasmas [9]. In accordance with this hypothesis, RMP ELM suppression has not been definitively observed in counter-rotating plasmas.

It is worth noting that there remains uncertainty in the interpretation of the experimental results due to the lack of toroidally resolved measurements. Specifically, it is unknown whether and to what extent the temperature perturbations measured by Thomson scattering, for example, are due to a helical distortion of the plasma, or to an axisymmetric change in the underlying equilibrium. The method of rotating the toroidal phase of the applied fields to explore the non-axisymmetric structure of the plasma assumes that the underlying axisymmetric equilibrium is largely independent of the phase. However, axisymmetric measures of the plasma equilibrium (such as line-averaged density and toroidal rotation) are found to be sensitive to the phase of the applied fields in practice. This indicates either the presence of significant error fields or the action of plasma control systems responding to toroidally localized measurements. Two results presented here suggest that the edge displacements are largely helical in nature: first, the displacements calculated by M3D-C1, which are purely helical, are in good agreement with the observed displacements; and second, the poloidal structure of the x-ray emission is strongly indicative of field-aligned helical structures. Ultimately, additional analysis of experimental measurements will be required to determine to what extent, and under what conditions, the helical response is greater than the axisymmetric response.

While these results indicate that the displacement is likely helical in character, the axisymmetric changes to the equilibrium induced by the application of non-axisymmetric fields — in particular, density pump-out and the braking of toroidal rotation — are often substantial, and may have important consequences for fusion energy output. Models of

neoclassical toroidal viscosity that take into account the response of the plasma are now being used to estimate the torque expected from non-axisymmetric perturbations [18, 19]. Models of transport in non-axisymmetric fields are also under development [20, 21]. Some of these models are presently being adapted to take the non-axisymmetric fields calculated with M3D-C1 as input.

This work was supported by the US Department of Energy under DE-FG02-95ER54309, DE-FG02-05ER54809, DE-AC02-09CH11466, and DE-AC05-00OR22725.

References

[1] A.M. Garofalo, *et al.*, *Phys. Rev. Lett.* **101** (2008) 195005
[2] T.E. Evans, *et al.*, *Phys. Rev. Lett.* **92** (2004) 235003
[3] S.C. McCool, *et al.*, *Nucl. Fusion* **29** (1989) 547
[4] J.C. Vallet, *et al.*, *Phys. Rev. Lett.* **67** (1991) 2662
[5] R.J. Buttery, *et al.*, *Nucl. Fusion* **51** (2011) 073016
[6] W. Fundamenski, R.A. Pitts, and JET EFDA contributors, *J. Nucl. Mater.* **363–365** (2007) 319
[7] N.M. Ferraro, *Phys. Plasmas* **19** (2012) 056105
[8] R.K.W. Roeder, B.I. Rapoport, and T.E. Evans, *Phys. Plasmas* **10** (2003) 3796
[9] P.B. Snyder, *et al.*, *Phys. Plasmas* **19** (2012) 056115
[10] M.R. Wade, *et al.*, in *Proc. of the 24th IAEA Fusion Energy Conf.*, San Diego, CA (International Atomic Energy Agency, 2012).
[11] R. Fitzpatrick, *Nucl. Fusion* **33** (1993) 1049
[12] E. Nardon, *et al.*, *Nucl. Fusion* **50** (2010) 034002
[13] M.W. Shafer, *et al.*, *Plasma and Fusion Res.* **6** (2011) 2402041
[14] R. Fitzpatrick and T.C. Hender, *Phys. Fluids B* **3** (1991) 644
[15] F.L. Waelbroeck, *Nucl. Fusion* **49** (2009) 104025
[16] M.F. Heyn, *et al.*, *Nucl. Fusion* **48** (2008) 024005
[17] D.M. Orlov, *et al.*, *Fusion Eng. and Design* **87** (2012) 1536
[18] J.-K. Park, *et al.*, *Phys. Plasmas* **16** (2009) 056115
[19] K. Kim, *et al.*, *Phys. Plasmas* **19** (2012) 082503
[20] J.D. Callen, *et al.*, *Nucl. Fusion* **52** (2012) 114005
[21] T.M. Bird and C.C. Hegna, A model for microinstability destabilization and enhanced transport in the presence of shielded 3-D magnetic perturbations. submitted to *Nucl. Fusion* (2012).